# Molecular Dynamics Simulations of Interactions between Polyanilines in Their Inclusion Complexes with $\beta$-Cyclodextrins

Syamal S. Tallury,[†,‡] Margaret B. Smyth,[§] Enes Cakmak,[†,‖] and Melissa A. Pasquinelli*[,†,§]

[†]Fiber and Polymer Science, North Carolina State University, Raleigh, North Carolina 27695, United States
[‡]Materials Science and Engineering, North Carolina State University, Raleigh, North Carolina 27695, United States
[§]Textile Engineering, North Carolina State University, Raleigh, North Carolina 27695, United States
[‖]Textile Engineering, Suleyman Demirel University, Isparta, Turkey

**ABSTRACT:** Conductive polymers have several applications such as in flexible displays, solar cells, and biomedical sensors. An inclusion complex of a conductive polymer and cyclodextrin is desired for some applications such as for molecular wires. In this study, different orientations of $\beta$-cyclodextrin rings on a single polyaniline (PANI) chain in an alternating emeraldine form were simulated using molecular dynamics. The simulations were performed in an implicit solvent environment that corresponds to experimental conditions. When the larger opening of the $\beta$-cyclodextrin toroids face the same direction, the cyclodextrins tend to repel each other. Alternating the orientation of the $\beta$-cyclodextrins on the chain causes the $\beta$-cyclodextrin rings to be more attractive to one another and form pairs or stacks of rings. These simulations explain how the $\beta$-cyclodextrins can be used to shield the polyaniline from outside chemical action by analyzing the PANI/cyclodextrin interactions from a molecular perspective.

β-Cyclodextrin ring orientations in
Inclusion Complexes with Polyaniline

Head-to-tail          Head-to-head
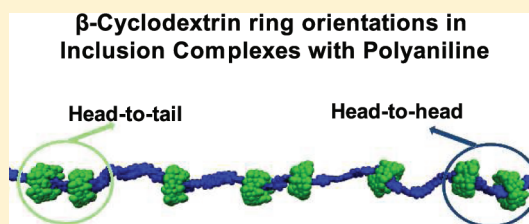
## INTRODUCTION

Conductive polymers are of interest because of their commercial use in electronics applications as light emitting diodes,[1] thin-film field effect transistors,[2] photovoltaic cells,[3] sensors,[4,5] and batteries.[6] Polyaniline (PANI) is a conjugated polymer that has been widely used for applications in organic electronics.[7] PANI is part of the semiflexible rod polymer family. Its chemical structure is given in Figure 1. Polymerized
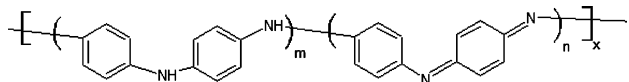
**Figure 1.** Chemical structure of PANI. For the emeraldine base form of PANI, $m = n$; thus, the structure is partially oxidized.

from the aniline monomer, PANI can be found in one of three idealized oxidation states, which impacts its overall conductivity. Emeraldine is the partially oxidized structure (where $n$ and $m$ in Figure 1 are 1:1), which becomes a conducting polymer when doped with an acid, and is highly stable at room temperature. Both the fully oxidized (pernigraniline) and the fully reduced (leucoemeraldine) forms are poor conductors, even when doped.

Insulated molecular wires derived from conductive polymers such as PANI can be created through the inclusion complex (IC) formation, where the polymer chain is encased non-covalently by another molecular species. ICs that involve conjugated polymers have chemical stabilities, reactivities, electrical conductivities, and luminescence different from bare

conjugated polymers.[8] Fabrication of these insulated molecular wires is possible via threading polymer chains within the macrocyclic substance or through the polymerization of monomer units of the inclusion complex. ICs are synthesized with certain solvents and under specific temperature conditions.[8]

One such macrocyclic substance that is used for IC formation is cyclodextrin (CD). CDs are cyclic oligosaccharides; $\alpha$-, $\beta$-, and $\gamma$-CD are made up of 6, 7, and 8 glucose units, respectively, joined by $\alpha$-1,4-glycosidic linkages with inner diameters of 0.5 to 1 nm and an outer diameter of 1.4−1.7 nm. The chemical structure of the $\beta$ form is given in Figure 2; it has an inner diameter of 6.0−6.5 Å. The CD molecules have a three-dimensional structure of a truncated cone toroid, where the cavity is hydrophobic and the outer surface is hydrophilic. Recent simulations suggest that the $\beta$-CD structure is more rigid than its $\alpha$ and $\gamma$ counterparts.[9] The self-assembly of CDs in the presence of a monomer or polymer species facilitates the formation of nanostructured ICs,[10,11] which are governed by the van der Waals forces, hydrophobic interactions, and hydrogen bonding between CD rings.[11−16] These nanostructures can be utilized to improve the mechanical and electrical properties of a material.[10,11,17] Inclusion complexation with CD rings are introduced not only for molecular wires[8] but also as a route to applications such as drug delivery,[18] robust polyrotaxane formation techniques,[15,19,20] and electron transfer
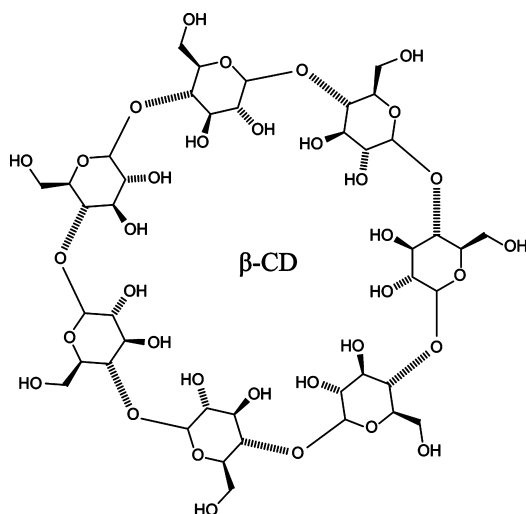
**Figure 2.** Chemical structure of β-CD.

reaction sites,[21] to name a few. Recent studies have demonstrated the molecular level insulation using CDs with polarizable conducting polymers as guest molecules.[22] In addition, the doped form is preferred to be formed prior to IC formation due to the insulating effects of the CD rings.[23]

Previous experimental studies have confirmed the threading of PANI molecules into β-CD cavities.[23−25] PANI complexation with the CDs can constrict the random movement of the polymer chains and induce an order and orientational effect into the bulk of the polymer species.[26] ICs between PANI and β-CDs are documented more widely[24,27,28] than with α- and γ-CDs, but PANI/β-CD ICs pose significant difficulties in characterization using crystallographic and thermal analysis techniques.[24] Because of the small size of its cavity, α-CD was not observed to form an IC with PANI, but molecular bundles of this molecule were observed to form a complex with PANI.[29] Inclusion was observed around 273 K for unmodified CD complexes.[24,28] Wang and coworkers synthesized and characterized a PANI/β-CD IC through polymerization in a supercritical $CO_2$ environment.[30] These ICs was used to improve dispersion in other polymers.[31,32] The effects of β-CD on the PANI structure was hypothesized to produce a rod-like structure,[26] and the linearity of PANI increases with an increase in the number of CD rings in the IC.[24] In addition, IC formation was observed to provide electrical insulation[33,34] and also an increase in the polarizability of PANI.[33] IC formation with β-CDs has been observed with solvents such as DMSO and water for CD and NMP for PANI, respectively. However, many questions remain on how solvents impact the PANI/β-CD threading behavior.

Computational studies have been performed on inclusion complexation with CDs,[35−38] even from very early stages of computational research.[39] Previous computations on PANI/CD complexes have reported that the geometry of PANI in a 1:1 stoichiometry complex in the fully oxidized form with β-CD in an IC is planar.[40] These QM-MM calculations also revealed that there is limited charge transfer between the PANI and β-CD and that the electronic structure of PANI is minimally impacted by the presence of the CDs; similar results were also obtained for other polymer ICs.[41] In contrast, modeling of a PANI/α-CD complex was predicted to reduce the electric conductance of PANI because of steric hindrance and molecular stabilization of the chains.[33] Quantum chemistry

calculations also revealed that doped PANI can be stabilized through IC formation by cross-linking α-CDs.[42] In comparison, experimental studies have observed the extended conformation of the polymer and have also indicated that CD can act as a dopant and can alter the electronic properties of PANI.[43]

The goal of this work is to study the interactions among individual β-CD molecules along a single PANI polymer chain in the emeraldine form with molecular dynamics (MD) simulations. In contrast to previous computational studies, the CD coverage of interest is significantly less than 1:1, specifically when there is approximately 1 CD ring per 4 repeat units of the polymer. MD simulations were used to identify the conformational behavior and molecular details of the PANI/β-CD ICs under various dielectric conditions.[42] Specifically, these simulations address the following research questions: (1) which orientation of β-CD toroids along a single PANI emeraldine chain is the most stable, head-to-head (HH) (and consequently, tail-to-tail) or head-to-tail (HT); (2) how is the orientation of β-CD rings affected by the rigidity of the chain conformation; and (3) how are the β-CD orientations and dynamics along the PANI chain impacted by the dielectric of the solvent environment? Therefore, we decoupled the effects of several factors, including the orientation of CDs relative to each other on the chain, the initial spacing of the rings along the chain, the effect of the solvent dielectric, and the effect of chain disorder. These results can be used by experimentalists to optimize their system through changes to the solvent conditions and are not only interesting from a molecular electronics perspective but also potentially for the design of molecular motors.

## ■ METHODOLOGY

**Molecular Models.** Molecular structures were built and refined with the Discover module of Materials Studio version 5.0[44] on Dell Optiplex 880 workstations. The structure of PANI of the emeraldine form (depicted in Figure 1) was built in the linear conformation with 48 repeat units in the head-to-tail configuration and was generated as an alternating copolymer of both of the monomer types. The molecular structure for β-CD (depicted in Figure 2) was obtained from the protein data bank,[45] entry 2Y4S.[46] The CD molecule was subjected to an energy minimization where the force tolerance was set to $10^{-6}$ amu Å/fs$^2$. Partial charges were assigned to cyclodextrin and PANI atoms from the PCFF force field.

The inclusion complex was created by first aligning the PANI chain along the $Z$ axis. Two types of simulations were run, one with the PANI chain held linear and the other with the PANI chain relaxed for 10 ps during the simulation; the chain relaxation introduces bending and kinks in the backbone as would be expected in a real system. A total of 14 β-CD molecules were built around the PANI chain. To investigate the effect of initial stacking distance, two different initial ring separations were created: one set where the rings are 25 Å apart from each other, and the other with the rings spaced regularly throughout the PANI chain. In each case, the systems were built with the β-CD molecules oriented in two different directions, as depicted in Figure 3: head-to-head (HH) and head-to-tail (HT).

**Molecular Dynamics (MD) Simulations.** MD simulations were performed with the LAMMPS molecular dynamics package.[47] An isochoric/isothermal (NVT) ensemble was used and the temperature was set to 300 K; the box was defined to be rectangular with 115 × 115 × 400 Å$^3$ edges.
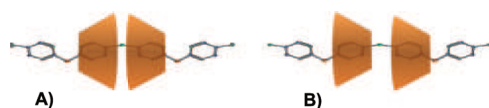
**Figure 3.** Possible orientations of the truncated conic toroids of the $\beta$-CD molecules in a polymer inclusion complex; (A) head-to-head (HH) and (B) head-to-tail (HT).

Cubic periodic conditions and zero pressure were applied. All systems were minimized initially using a energy tolerance of $1.0 \times 10^{-3}$ and a force tolerance of $1.0 \times 10^{-4}$. A time step of 1 fs was used, and a production run time of 1 ns was set for all simulations. All bonded interactions including bonds, angles, dihedrals, and impropers were defined with the quartic style of the PCFF force field,[48] which was previously reported to have accurate results for such systems.[49−51] The Debye screening method was employed to replicate an implicit (dielectric based) solvent environment. The Debye length was set to 1.4 Å$^{-1}$, whereas the dielectric effects were studied for dielectric values of 1, 40, 80, and 160. Lennard-Jones potentials were used to replicate the nonbonded interactions. The cutoff for the nonbonded interactions was optimized by varying it up to 15 Å; the optimal value was thus determined to be 10.0 Å due to negligible changes beyond that value. The equilibration and minimization runs were performed on Sun Ultra 40 M2 Workstations with Fedora Core 8 under serial mode. The production runs were performed on 8 processors each under parallel mode at the NC State High Performance Computing facility.

## RESULTS AND DISCUSSION

The goal of this work is to investigate a $\beta$-CD inclusion complex with the emeraldine base form of PANI in a system where the coverage was significantly less than 1:1, specifically when there is approximately 1 CD ring per 4 repeat units of the polymer. Our focus was on how the stacking of the $\beta$-CD toroids along the chain is impacted by the dielectric of the solvent. We investigated the different orientations of the toroids along the chain; as depicted in Figure 3, these orientations are defined as either head-to-head (HH) (and consequently, tail-to-tail) or head-to-tail (HT).

Recent work has identified that the orientation of these toroids impact the formation and stability of CD ring stacks, particularly in the presence of an inclusion compound and solvent.[19,20] From ab initio and semiempirical (MNDO/PM3) calculations, the HT dimer conformation was predicted to be

more thermodynamically stable.[52] In addition, binding free energies calculated with MM-PBSA suggest that the $\beta$-CD toroids are likely to exist in the form of monomers in solution, unlike the smaller $\alpha$-CDs.[53] However, MD simulations with the AMBER force field predicted that the HH orientation is the most stable for $\beta$-CD in vacuum due to the large number of intermolecular hydrogen bonds that are formed, although in an aqueous environment, the TT configuration was predicted to be more stable for $\beta$-CD.[53,54] Thus, the solvent can play an important role in dictating the preferred orientation of the $\beta$-CD toroids during inclusion complex formation.

PANI belongs to the semiflexible rod family; for the emeraldine base form, the partially oxidized and electrically conducting form, the rings deviate from planarity approximately by ±30°,[55,56] but otherwise, it is expected to have a fairly linear chain conformation, especially in a good solvent.[57] In our simulations, we have three configurational settings: (1) the PANI chain can be either linear or in a relaxed (kinked) form, (2) the $\beta$-CD rings can be either closely stacked or spread out throughout the PANI chain length, and (3) the orientational variation of the $\beta$-CD rings relative to one another (HT versus HH in Figure 3).

MD simulations in the NVT ensemble were performed on a single chain of PANI in the emeraldine form, which is complexed with 14 $\beta$-CD molecules that are oriented in both HH and HT configurations. (Note that the alternating pairs of $\beta$-CDs in HH take up head-to-head and then tail-to-tail association in this configuration.) In addition, two starting configurations were tried, one where initially they are spaced close together, and one where they are spaced far apart. The simulations are initially performed with the chain being frozen in its linear but not planar structure, and then they are repeated with chain relaxation, and thus kinks can occur within the PANI chain. By holding the chain fixed in a linear conformation, the molecular motion of the $\beta$-CD molecules can be decoupled from the molecular motions of PANI.

Debye screening was also applied to investigate how the behavior of the $\beta$-CDs may change in different dielectric environments; dielectric ($\varepsilon$) values of 40, 80, and 160 were used. Implicit solvent via Debye screening was used because it is assumed that the main effect of the solvent is to shield the electrostatic interactions and that the effects of viscosity are expected to be consistent across the series of solvents that are of interest. Thus, an understanding of the effect of solvent dielectric on the properties of the $\beta$-CD/PANI IC will help experimentalists determine solvents that may produce the desired IC characteristics.
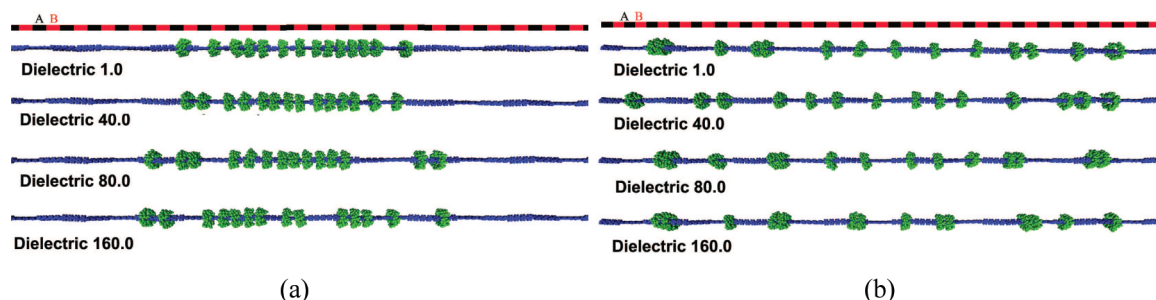


**Figure 4.** MD snapshots at 1 ns of PANI/$\beta$-CD complexes in the HT configuration in three different dielectric media and with a fixed linear chain of PANI. (a) The rings were initially spaced close to each other, and (b) the rings were initially spaced far apart from each other. All $\beta$-CD rings are colored green, and the PANI chain is colored blue. The red and black bar at the top indicates where each oxidation form (from Figure 1) is located within the chain.
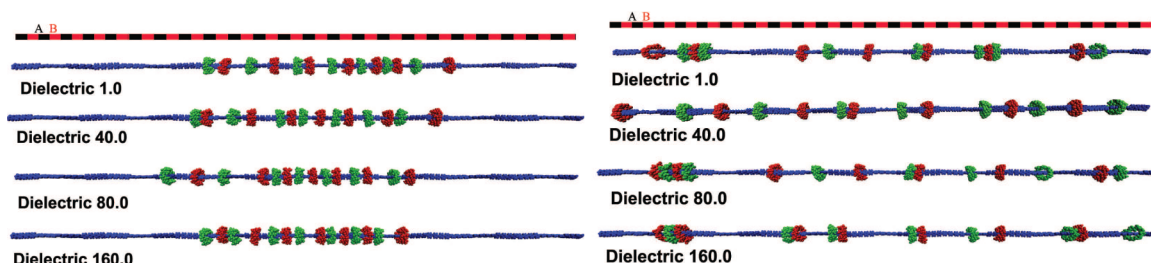
**Figure 5.** Same as that in Figure 4, except for the HH configuration of β-CD rings; the rings facing toward the positive Z axis are colored green, and others are colored red; the PANI chain is colored blue.

**Table 1. Properties Extracted from the MD Simulations of the CD Configurations Where They Were Initially Spread Apart along a Linear Polyaniline Chain As a Function of Solvent Dielectric**[a]

| | | | | | preferred unit | |
|---|---|---|---|---|---|---|
| $\varepsilon$ | type | potential energy (kcal/mol) | Coulombic energy (kcal/mol) | $E_{inter}$ (CD/PANI) (kcal/mol) | A | B |
| 1 | HT | 3822 ± 43 | −73.7 ± 6.4 | −357 ± 10 | 1.32 | 0.68 |
| | HH | 3518 ± 39 | −69.5 ± 4.3 | −346 ± 14 | 1.05 | 0.95 |
| 40 | HT | 5857 ± 42 | −1.7 ± 0.4 | −417 ± 1 | 1.21 | 0.79 |
| | HH | 5420 ± 50 | −1.7 ± 0.3 | −409 ± 4 | 0.94 | 1.06 |
| 80 | HT | 5840 ± 37 | −0.9 ± 0.4 | −426 ± 9 | 1.15 | 0.85 |
| | HH | 5670 ± 31 | −0.9 ± 0.2 | −412 ± 9 | 1.00 | 1.00 |
| 160 | HT | 5893 ± 24 | −0.5 ± 0.3 | −419 ± 7 | 0.93 | 1.06 |
| | HH | 5760 ± 25 | −0.4 ± 0.3 | −420 ± 9 | 0.90 | 1.10 |

[a]See text for details on the preferred unit column.

**Linear PANI Chain.** Snapshots from the MD simulations where the β-CD rings were built closely spaced in the HT configuration in the three different dielectric media are given in Figure 4a. For $\varepsilon = 1$, which is vacuum conditions, the β-CD rings are observed to interact strongly with each other, leading to good association with their neighboring rings, and thus, a congregated group of rings is observed toward the middle of the polymer chain. Although some rings are observed to pair up, there are stacks of β-CD rings with strong interactions with others on either side. For $\varepsilon = 40$, a similar observation is made to the vacuum conditions. For $\varepsilon = 80$, the rings spread out wider than for $\varepsilon = 40$ but stacks of several rings are still prevalent. For $\varepsilon = 160$, increased distance between the consecutive rings is observed. This trend suggests that the HT configuration of β-CDs is overall attractive, and the differences observed as $\varepsilon$ is increased are due to the shielding effect of the dielectric medium. In a lower dielectric medium, the charges on the β-CD molecules can feel those on the neighboring rings, but that effect is dramatically reduced as the dielectric value increases in magnitude, hence the observation that the rings are spread apart as the simulation progresses. For the system where the initial configuration of β-CD molecules was widely spaced apart (Figure 4b), most of the β-CD rings remain spaced uniformly throughout the polymer chain in all four dielectrics, although a few ring groups are observed. It is noteworthy that the cutoffs for the nonbonded interactions are below the initial separation between any two β-CD rings in this case, although some rings do eventually find other CDs. No obvious trend with dielectric is observed in this case.

For the HH configuration of the β-CDs on a linear chain, the results are given in Figure 5. For the case where the β-CDs were initially closely spaced (Figure 5a), the trend with the dielectric is opposite to that observed for the HT configuration in Figure 4a; in other words, as the dielectric increases, the β-CDs are observed to remain closer to each other rather than

spread apart. This observation suggests that the HH configuration (and, consequently, the TT configuration) tends to be more repulsive than the HT configuration. As the dielectric is increased, that repulsion is weakened, which results in the β-CD molecules remaining relatively close to one another. However, for the system where the rings were initially well-spaced in Figure 5b, some pairwise associations with a neighboring ring are observed but no ring stacks. No obvious trend with dielectric is observed in this case.

As the PANI chain in our simulations is comprised of two alternating oxidation states (Figure 1), there is the possibility that the β-CD rings may have a preference for one oxidation state over another, which we will refer to the A versus B form. From the snapshots of the linear chain simulations in Figures 4 and 5, the β-CD rings seem to not have a preference of interacting with the A form over the B form in both the HT and HH configurations. We calculated a time averaged value over the entire simulation trajectory for the amount of rings on each oxidation form by first calculating at each time step the number of β-CD atoms located around the A or B form (no double counting of CD atoms is done) divided by the total number of atoms in an entire β-CD ring. These values were then summed over all A and B forms within the chain, and then averaged over the entire trajectory. The average values were then normalized by dividing by 7. Thus, if the β-CD rings have no preference for one of the two oxidation states, the resulting normalized count will be 1.0 for both the A and B form. A number of more than one indicates a preference for that oxidation state form, whereas a number of less than one indicates that the β-CD ring was not as preferred on that oxidation state form.

The values for the preference of the β-CD rings for the different oxidation forms in PANI for the systems in Figures 4 and 5 are given in Table 1. These values suggest that the β-CD rings were preferentially interacting with A in the HT configuration, which can be attributed to favorable electro-
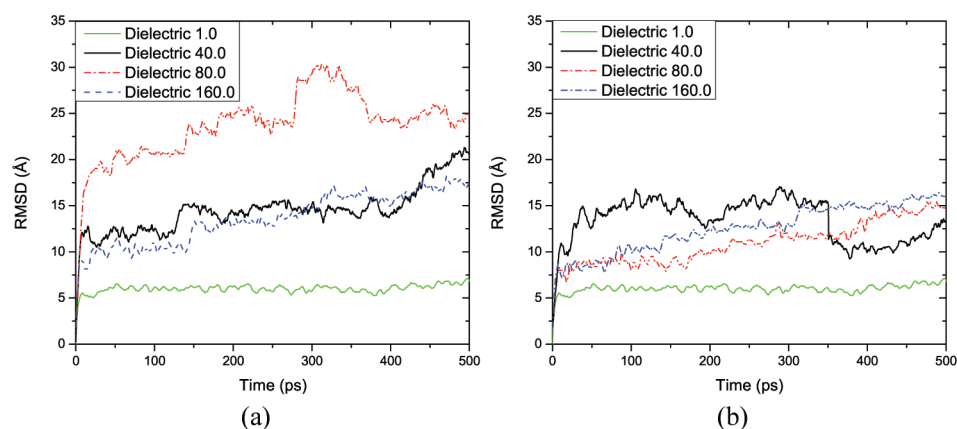
2026

dx.doi.org/10.1021/jp206745q | J. Phys. Chem. B 2012, 116, 2023–2030

**Figure 6.** Average rmsd of the CD rings in the initially spread out configuration for the linear PANI chain as a function of time. The configurations of β-CDs are (a) HT and (b) HH. The blue dotted line is for ε = 160, the red dotted line is for ε = 80, the black solid line is for ε = 40, and the green solid line is for ε = 1.0.
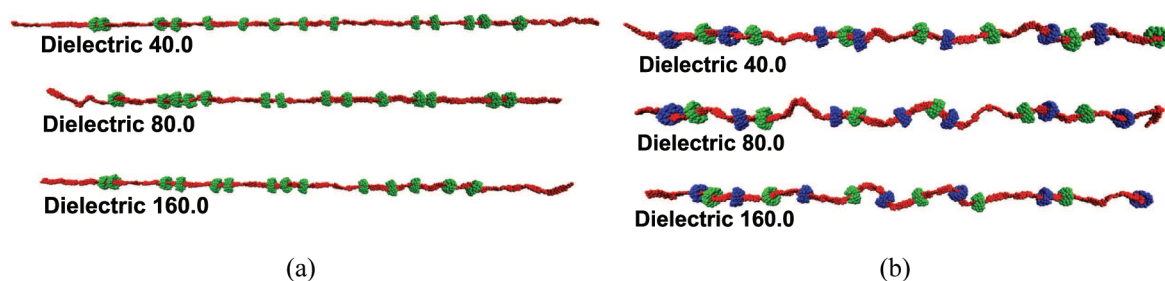


**Figure 7.** MD snapshots at 1 ns of PANI/β-CD complexes in three different dielectric media and with a relaxed linear chain of PANI in the (a) HT configuration and (b) HH configuration. In the initial structure, the β-CD rings were spaced far apart.

statics due to the electronegative hydrogen atom on the amine group in that oxidation state (Figure 1). This effect is strongest in the vacuum conditions (ε = 1), and this effect diminishes as the dielectric increases to 160, confirming the electrostatic nature of these interactions. In the HH configuration, no strong preference between the oxidation states is observed, although for ε = 160, the B form appears to be slightly preferred.

*System Energies.* Table 1 contains the energies of the β-CDs/PANI systems with the linear polymer chain where the rings are initially spread apart. The HH configurations are lower in potential energy overall as compared to the HT in all of the dielectric media, which can be attributed to the interaction among the β-CD rings providing more energetic stability. The potential energies for the vacuum conditions are the lowest in both the HH and the HT configurations. As the dielectric is increased, the potential energies increase due to the overall decrease in electrostatic interactions due to the significantly lower Coulombic energies from the Debye screening. For the HT configurations, the values do not significantly change for the nonvacuum dielectric values, but it does for the HH configurations, where the potential energy is lowest for ε = 40.

The interaction energy between the PANI chain and the β-CD rings does not seem to vary significantly at higher dielectric values; however, the interaction energy is significantly lower for the vacuum conditions due to the Debye screening effects. This change could also suggest a shift of the interaction among β-CD rings to the interaction between the polymer and β-CD rings with the application of higher dielectric values. There is also no obvious trend in the interaction energies with respect to the orientation of the β-CD rings.

*Dynamics of β-CD Rings.* In general, we observed that the majority of the movements of the β-CDs were from the rings spinning around the PANI chain rather than along the length of the polymer for all dielectrics and starting conformations. Figure 6 provides the root mean squared displacement (rmsd) as a function of simulation time of the β-CD rings (based on the locations of the ether oxygens) starting from a spread out conformation from the simulations with a linear PANI chain. The β-CDs were observed to move in pairs or stacks while having lots of space between them. The comparison between the rmsd for HT configurations in Figure 6a indicates that as a function of dielectric, the motions increase overall as the attraction among rings decreases (note that each β-CD ring feels attraction from neighboring rings on both sides). Since 48 repeat units of PANI is 810 Å in this linear conformation, less than 1% of the chain is explored by each ring for the lower dielectrics and vacuum conditions. In contrast, for the higher dielectrics, each ring explores about 2−3% of the chain. This observation suggests that the attraction among the rings keeps the β-CDs more localized, and as the attraction is shielded by the dielectric, more motion along the chain is possible, and thus, their motion becomes more delocalized, as supported by the decrease in the oxidation form preference but no change in the overall interaction energies with the PANI chain in Table 1.

Similar observations can be made for the HH configurations in Figure 6b. However, in contrast to HT, the configurations at higher dielectrics all have a similar rmsd value of 15 Å at the end of the simulation, or about 2% of the chain. It can be inferred from this observation that the repulsion in this configuration provides some stability in terms of the overall spacing and motions of the β-CDs along the chain that is not
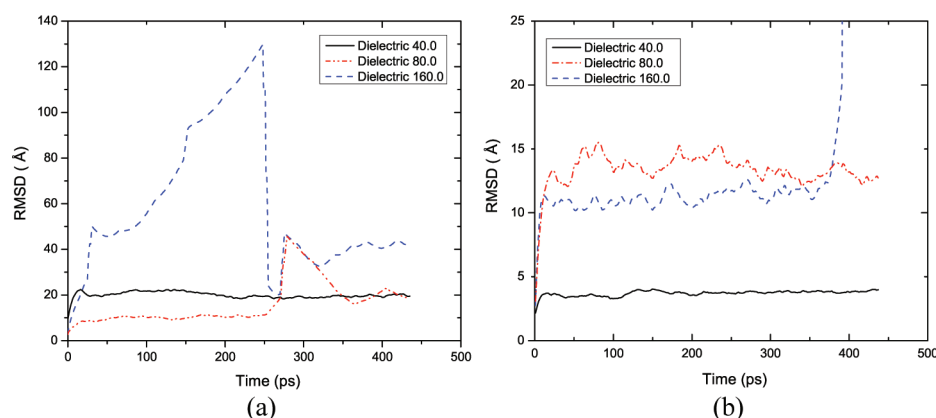
**Figure 8.** Same as that in Figure 6 but for the relaxed PANI chain.

significantly impacted by the dielectric. For the initial configuration where the $\beta$-CDs were more closely spaced for both the HH and HT configurations (results not shown), the motion was much less significant, particularly as a function of the dielectric.

**Relaxed PANI Chain Results.** These linear chain simulations indicate that during the course of the simulations, the $\beta$-CD rings come under the influence of each other and settle into energetically favorable conformations, which are dependent on the dielectric environment for just the HH configurations. However, the chain conformation of the host guest polymer chain can also impact the interactions between the $\beta$-CDs. To investigate the effect of polymer chain irregularities, these simulations were repeated with a relaxed PANI chain. When the PANI chain is relaxed for the first 10 ps of each simulation, the polymer chain develops kinks along the backbone. This set of simulations provides information about the effect of chain irregularity on the $\beta$-CD interactions. The initial structures were created such that the $\beta$-CD rings are spaced far apart, and MD snapshots of the final configurations are given in Figure 7.

For the HT configuration in Figure 7a, the nonlinearity of the backbone is more pronounced in the simulations with the dielectric of 80 and 160, although the disorder is minimal. In addition, the rings were observed to remain separated for $\varepsilon = 40$, and to start stacking with an increase in $\varepsilon$. This observation is in agreement with the trend that was observed in the linear chain simulations (Figure 4b). Some differences, however, were observed due to the kinks along the PANI chain. Specifically, the degree of stacking increased with an increase in $\varepsilon$, which is likely due to the confinement of the rings from the randomly positioned kinks along the PANI chain. Such an observation suggests that the nonlinear conformation of the PANI chain can result in significant changes in the $\beta$-CD interactions.

The motion of $\beta$-CD rings along the PANI chain was hindered due to the presence of kinks, and the $\beta$-CD rings were stuck on certain segments of the backbone; many $\beta$-CD rings were observed to have very good interaction with adjacent CD molecules despite the bending in the backbone. For the HH configurations in Figure 7b, more kinks were formed than in the HT case for all three dielectrics. The reason for this difference as a result of the orientation of $\beta$-CD rings could be because there is significant motion of CDs in the HT configuration during the relaxation process, whereas there is a restricted motion due to more stable HH ring–ring attractions. However, as $\varepsilon$ increased, the chain bending became more

pronounced and thus restricted some of the $\beta$-CD rings from crossing over the kinks. Hence, the rings never explore interactions with a ring on the other side of the kink except through the formation of a loop in the chain, such as is observed in the middle of the $\varepsilon = 160$ chain. This observation indicates that the HH interaction is the least favorable between the $\beta$-CD molecules even if the PANI chain is in a nonlinear conformation.

*Dynamics of $\beta$-CD Rings.* The rmsd of the ether oxygen atoms in the $\beta$-CD rings as a function of time for the HT configuration is given in Figure 8a. For $\varepsilon = 40$, the $\beta$-CD rings are more stable due to significant interactions with the neighboring rings. In $\varepsilon = 80$, for a long duration in the initial stages, the $\beta$-CD rings exhibit motion along approximately 2% of the chain; however, after 260 ps, there is a sudden rise in the motion of the rings, which recedes to a lower rmsd value later. The sudden peak in the rmsd plot can be attributed to the escape of a $\beta$-CD ring from the terminus of the PANI chain. For $\varepsilon = 160$, the rmsd values are much larger, and a substantial increase in rmsd above 100 Å is noticed at about the 160 ps frame. These larger values of rmsd are attributed to the escape of a ring from the IC and its motion in the MD cell. No obvious trend is observed in these HT simulations as a function of the dielectric medium.

However in the HH configuration in Figure 8b, a regular trend is observed with respect to the dielectric of the medium. The overall rmsd of $\beta$-CD oxygens is significantly lower than in the HT configurations for all three dielectric values. The rmsd values are lowest for $\varepsilon = 40$; throughout the simulations, the rmsd value remains below 5 Å, suggesting that there is low overall translational motion of the rings due to the kinks. The rmsd for $\varepsilon = 80$ and 160 are comparable and are below 15 Å for most of the simulation time. There is a sudden peak observed in $\varepsilon = 60$ close to 400 ps again due to the escape of a CD molecule from the IC.

**Correlations to Experiments.** The broad range of dielectric constants from 40 to 160 used in these simulations mimic solvents in experimental conditions such as DMSO, water, and NMP. Although recent models[40] predict 1:1 complexation of PANI and $\beta$-CDs during IC formation, recent experiments provide evidence that the threading of $\beta$-CD does not produce a high yield of coverage of PANI with pristine $\beta$-CDs (0.07−0.2 CDs per repeat unit[58]). These simulations mimic the conditions of low density complexation, and the unthreading of CD rings is even observed in Figure 8a.

## CONCLUSIONS

The results of these MD simulations on PANI/$\beta$-CD ICs with partial coverage indicate (1) that the $\beta$-CDs tend to be more attractive in the HT configuration and more repulsive in the HH configuration, which is impacted by a dielectric; (2) that the translational motion of the rings along the chain is on the order of 1−3% of the chain, the latter of which is for the HT configuration in higher dielectrics, (3) that the HT configuration has a lower potential energy than HH configuration in all dielectrics, and (4) that kinks in the chain reduce the motion of the $\beta$-CD rings due to confinement effects.

## AUTHOR INFORMATION

**Corresponding Author**
*E-mail: melissa_pasquinelli@ncsu.edu.

## ACKNOWLEDGMENTS

## REFERENCES

(1) Gustafsson, G.; Cao, Y.; Treacy, G. M.; Klavetter, F.; Colaneri, N.; Heeger, A. J. *Nature* **1992**, *357*, 477−479.
(2) Paloheimo, J.; Kuivalainen, P.; Stubb, H.; Vuorimaa, E.; Yli-Lahti, P. *Appl. Phys. Lett.* **2009**, *56*, 1156−1159.
(3) Hoppea, H.; Sariciftci, N. S. *J. Mater. Res.* **2004**, *19*, 1924−1945.
(4) Partridge, A. C.; Harris, P.; Andrews, M. K. *Analyst* **1996**, *121*, 1349−1353.
(5) Gerard, M.; Chaubey, A.; Malhotra, B. D. *Biosens. Bioelectron.* **2002**, *17*, 345−359.
(6) Scrosati, B. *Polym. Int.* **1998**, *47*, 50−55.
(7) Ameen, S.; Akhtar, S.; Husain, M. *Sci. Adv. Mater.* **2010**, *2*, 441−462.
(8) Frampton, M. J.; Anderson, H. L. *Angew. Chem., Int. Ed.* **2007**, *46*, 1028−1064.
(9) Naidoo, K. J.; Gamieldien, M. R.; Chen, J. Y.-J.; Widmalm, G.; Maliniak, A. *J. Phys. Chem. B* **2008**, *112*, 15151−15157.
(10) Tonelli, A. In *Inclusion Polymers*; Advances in Polymer Science; Wenz, G., Ed.; Springer: Berlin, Germany, 2009; Vol. 222, pp 115−173.
(11) Wenz, G. In *Inclusion Polymers*; Advances in Polymer Science; Wenz, G., Ed.; Springer: Berlin, Germany, 2009; Vol. 222, pp 1−54.
(12) Galant, C.; Kjøniksen, A.-L.; Nguyen, G. T. M.; Knudsen, K. D.; Nyström, B. *J. Phys. Chem. B* **2006**, *110*, 190−195.
(13) Harada, A.; Li, J.; Suzuki, S.; Kamachi, M. *Macromolecules* **1993**, *26*, 5267−5268.
(14) Al-Sou'od, K. *J. Inclusion Phenom. Macrocyclic Chem.* **2006**, *54*, 123−127.
(15) Pozuelo, J.; Mendicuti, F.; Mattice, W. L. *Macromolecules* **1997**, *30*, 3685−3690.
(16) Pozuelo, J.; Nakamura, A.; Mendicuti, F. *J. Inclusion Phenom. Macrocyclic Chem.* **1999**, *35*, 467−485.
(17) Anitha, G.; Subramanian, E. *J. Polym. Sci., Part A: Polym. Chem.* **2006**, *44*, 281−294.
(18) Fronza, G.; Mele, A.; Redenti, E.; Ventura, P. *J. Org. Chem.* **1996**, *61*, 909−914.
(19) Anconi, C.; Nascimento, C.; De Almeida, W.; Dos Santos, H. *J. Inclusion Phenom. Macrocyclic Chem.* **2008**, *60*, 25−33.
(20) Anconi, C; Nascimento, C. S.; De Almeida, W. B.; Dos Santos, H. F. *J. Phys. Chem. B* **2009**, *113*, 9762−9769.
(21) Matsue, T.; Evans, D. H.; Osa, T.; Kobayashi, N. *J. Am. Chem. Soc.* **1985**, *107*, 3411−3417.
(22) Cacialli, F.; Wilson, J. S.; Michels, J. J.; Daniel, C.; Silva, C.; Friend, R. H.; Severin, N.; Samori, P.; Rabe, J. P.; O'Connell, M. J.; Taylor, P. N.; Anderson, H. L. *Nat. Mater.* **2002**, *1*, 160−164.
(23) Grigoras, M.; Stafie, L. *Supramol. Chem.* **2010**, *22*, 237−248.
(24) Yoshida, K.; Shimomura, T.; Ito, K.; Hayakawa, R. *Langmuir* **1999**, *15*, 910−913.
(25) Shimomura, T.; Akai, T.; Abe, T.; Ito, K. *J. Chem. Phys.* **2002**, *116*, 1753.
(26) Ding, Y.; Abdiryim, T.; An, S.; Nurulla, I. *J. Appl. Polym. Sci.* **2008**, *107*, 3864−3870.
(27) Subramanian, E.; Anitha, G.; Selvam, M.; Badusha, M. A. *Bull. Mater. Sci.* **2005**, *28*, 55−61.
(28) Yuan, G.; Kuramoto, N.; Takeishi, M. *Polym. Adv. Technol.* **2003**, *14*, 428−432.
(29) Shimomura, T.; Akai, T.; Fujimori, M.; Heike, S.; Hashizume, T.; Ito, K. *Synth. Met.* **2005**, *153*, 497−500.
(30) Wang, B.; He, J.; Sun, D.; Zhang, R.; Han, B.; Huang, Y.; Yang, G. *Eur. Polym. J.* **2005**, *41*, 2483−2487.
(31) Li, X.; Zhao, Y.; Zhuang, T.; Wang, G.; Gu, Q. *Colloids Surf., A* **2007**, *295*, 14−151.
(32) Prasannan, A.; Truong, T. L. B.; Hong, P.; Somanathan, N.; Shown, I.; Imae, T. *Langmuir* **2011**, *27*, 766−773.
(33) Taniguchi, M.; Kawai, T. *Chem. Phys. Lett.* **2006**, *431*, 127−131.
(34) Shimomura, T.; Yoshida, K.; Ito, K.; Hayakawa, R. *Polym. Adv. Technol.* **2000**, *11*, 837−839.
(35) Wang, T.; Cai, W. S.; Shao, X. G. *Prog. Chem.* **2010**, *22*, 803−811.
(36) Castro, E. A.; Barbiric, D. A. *J. Curr. Org. Chem.* **2006**, *10*, 715−729.
(37) Paik, Y.; Poliks, B.; Rusa, C. C.; Tonelli, A. E.; Schaefer, J. *J. Polym. Sci., Part B: Polym. Phys.* **2007**, *45*, 1271−1282.
(38) Chai, M.; Ravi, S.; Kujaski, M. P.; Rakesh, L. *Nanoparticles: Synthesis, Stabilization, Passivation,and Functionalization*; Nagarajan, R., Hatton, T. A., Eds; ACS Symposium Series; American Chemical Society: Washington DC, 2008; Chapter 28, pp 402−416.
(39) Behr, J. P.; Lehn, J. M. *J. Am. Chem. Soc.* **1976**, *98*, 1743−1747.
(40) Belosludov, R. V.; Mizuseki, H.; Ichinoseki, K.; Kawazoe, Y. *Jpn. J. Appl. Phys.* **2002**, *41*, 2739−2741.
(41) Belosludov, R. V.; Farajian, A. A.; Mizuseki, H.; Ichinoseki, K.; Kawazoe, Y. *Jpn. J. Appl. Phys.* **2004**, *43*, 2061−2063.
(42) Belosludov, R. V.; Farajian, A. A.; Kikuchi, Y.; Mizuseki, H.; Kawazoe, Y. *Comput. Mater. Sci.* **2006**, *36*, 130−134.
(43) Subramanian, E.; Anitha, G.; Selvam, M.; Ali Badusha, M. *Bull. Mater. Sci.* **2005**, *28*, 55−61.
(44) *Accelrys Software, C*; Accelrys: San Diego, 2004.
(45) Banerjee, A.; Mikhailova, E.; Cheley, S.; Gu, L.-Q.; Montoya, M.; Nagaoka, Y.; Gouaux, E.; Bayley, H. *Proc. Natl. Acad. Sci. U.S.A.* **2010**, *107*, 8165−8170.
(46) Vester-Christensen, M. B.; Hachem, M. A.; Svensson, B.; Henriksen, A. *J. Mol. Biol.* **2010**, *403*, 739−750.
(47) Plimpton, S. *J. Comput. Phys.* **1995**, *117*, 1−19.
(48) Maple, J. R.; Dinur, U.; Hagler, A. T. *Proc. Natl. Acad. Sci. U.S.A.* **1988**, *85*, 5350−5354.
(49) Melani, F.; Mura, P.; Adamo, M.; Maestrelli, F.; Gratteri, P.; Bonaccini, C. *Chem. Phys. Lett.* **2003**, *370*, 280−292.
(50) Yu, Y. M.; Cai, W.; Shao, X. *J. Inclusion Phenom. Macrocyclic Chem.* **2006**, *56*, 225−235.
(51) Vaia, R. A.; Dudis, D.; Henes, J. *Polymer* **1998**, *39*, 6021−6036.
(52) Avakyan, V. G.; Nazarov, V. B.; Alfimov, M. V.; Bagaturyants, A. A.; Voronezheva, N. I. *Russ. Chem. Bull.* **2001**, *50*, 206−216.
(53) Bonnet, P.; Jaime, C.; Morin-Allory, L. *J. Org. Chem.* **2002**, *67*, 8602−8609.
(54) Bonnet, P.; Jaime, C.; Morin-Allory, L. *J. Org. Chem.* **2001**, *66*, 689−692.
(55) Maron, J.; Winokur, M. J.; Mattes, B. R. *Macromolecules* **1995**, *28*, 4475−4486.
(56) Jozefowicz, M. E.; Laversanne, R.; Javadi, H. H. S.; Epstein, A. J.; Pouget, J. P.; Tang, X.; MacDiarmid, A. G. *Phys. Rev. B* **1989**, *39*, 12958−12961.

2029

dx.doi.org/10.1021/jp206745q | *J. Phys. Chem. B* 2012, 116, 2023−2030

(57) Avlyanov, J. K.; Min, Y.; MacDiarmid, A. G.; Epstein, A. J. *Synth. Met.* **1995**, *72*, 65−71.

(58) Grigoras, M.; Conduruta, D. G. *J. Inclusion Phenom. Macrocyclic Chem.* **2006**, *54*, 101−107.